Optical Properties of Oxygen Vacancies in Germanium Oxides: Quantum Chemical Modeling of Photoexcitation and Photoluminescence

A. S. Zyubin,*,†,‡ A. M. Mebel,§ and S. H. Lin†

Institute of Atomic and Molecular Sciences, Academia Sinica, P.O. Box 23-166, Taipei 106, Taiwan, Institute of Problems of Chemical Physics, Russian Academy of Sciences, Chernogolovka, Moscow Region 142432, Russia, and Department of Chemistry and Biochemistry, Florida International University, Miami, FL 33199

Received: March 23, 2007; In Final Form: May 22, 2007

Photoabsorption and photoluminescence properties of single and double oxygen vacancy (OV and DOV) defects in quartz-like germanium oxide have been investigated by high-level ab initio calculations. It has been found that photoabsorption for these systems occurs at lower energies as compared to the analogous defects in SiO_2. For OV, the lowest electronic excitations with high oscillator strengths have energies of 6.7−7.0 eV, whereas for DOV, the lowest-energy photoabsorption band is calculated to be in the range of 5.5−5.9 eV. Significant geometry relaxation and large Stokes shift are inherent for these excited states and, as a result, their photoluminescence bands are predicted to peak at 3.1−3.3 eV for OV and at 2.6 eV for DOV. The double oxygen vacancy is suggested to be the most suitable candidate for generating bright blue photoluminescence observed experimentally for substoichiometric quartz-like GeO_2 nanowires, as the calculated optical properties of DOV are in close agreement with the features found in experiment.

Introduction

Several years ago, bulk-quantity GeO_2 nanowires with a diameter of about 50−120 nm with remarkable photoluminescence (PL) properties were synthesized.[1] The chemical composition of these nano-objects is close to $GeO_{1.75}$ (substoichiometric GeO_2) with a quartz-like structure. The most significant characteristic of these nanowires is that, under photoexcitation (PE) at 5.6 eV, they emit stable and high-brightness blue light in the energy range between 2 and 3 eV with the peak position at 2.56 eV. The PL intensity for nanowires[1] was found to be more than an order of magnitude higher than for GeO_2 nanopowders.[2,3] The PL was speculated to originate from singlet−singlet transitions (S_0−S_1, S_0−S_2 or higher) at one or more point defects; however, the nature of the emitting centers is still unknown. It was proposed[1] that PL is related to electronic transitions at oxygen vacancies, but the observed PL band is rather broad and may have a multisource origin; at least several defects possessing photoabsorption (PA) near 5.5 eV can contribute to its formation if they have suitable PL properties.

PA properties of point defects in germanosilicate glasses and in pure SiO_2 and GeO_2 have attracted significant attention in recent years because of their potential applications in combined GeO_2/SiO_2 systems, such as optical fibers, second harmonic generation, and Bragg phase-grating formation, or interconnects and functional components of prospective mesoscopic electronic-optical devices.[4−11] The broad multisource PA band near 5 eV has drawn a special interest because it is likely to be associated with photostructural transformations and photosensitive grating effects.[4,11−19]

To date, PA properties of various point defects in SiO_2 have been systematically investigated using quantum chemical calculations,[4,20−30] which allowed a detailed and substantiated interpretation of available experimental data. On the other hand, analogous calculations of PA properties for GeO_2 defects are still scarce, but because of the similarity in the characteristics of point defects in SiO_2 and GeO_2, one can deduce reasonable estimates for the missing data. On this basis, we could gather that in quartz-like GeO_2 at least several point defects, :Ge< and O═Ge< groups, oxygen vacancy and divacancy (OV, DOV), peroxide radical −O−O−Ge≡, and surface E′−center−Ge≡, are able to contribute into the PA band near 5 eV. In addition to the requirement to absorb around 5 eV, in order to be considered as candidates to contribute to the bright blue luminescence in GeO_2 nanowires,[1] the defects should be able to produce PL in the appropriate energy range, near 2.5 eV, and have substantial oscillator strengths both for PA and PL transitions. Up to now, PL properties of both GeO_2 and SiO_2 point defects are much less understood, as theoretical calculations of these properties remain rather limited, mainly due to the difficulties with geometry optimization for excited electronic states in model clusters simulating point defects. Recently,[20,26,30,31] emission energies for some GeO_2 defects including :Ge<, O═Ge<, −O−O−Ge≡, −Ge≡, and a combination of OV with −Ge≡ were calculated, but none of them were found to have the suitable combination of the PA and PL properties.

The PL properties of oxygen vacancies (OV) and double vacancies (DOV), which are probable candidates to contribute to the PL band observed in nanowires,[1] have not been investigated in detail as of yet. Only photoabsorption energies were studied theoretically both for SiO_2 and GeO_2-related OVs.[21−24] For OV in SiO_2, the calculated vertical S_0−S_1 excitation energy, 7.0−7.5 eV, was in reasonable agreement with the experimental value of ~7.6 eV, but for GeO_2 OV, approximately the same energy was obtained,[21] and the result seems to be overestimated. A possible reason for this overestimation is the use of the 6-31G* basis set in the calculations both for Si and Ge. The quality of this basis set is not uniform,

* Corresponding author. E-mail: zyubinas@bk.ru.
† Academia Sinica.
‡ Russian Academy of Sciences.
§ Florida International University.

10.1021/jp072314f CCC: $37.00 © 2007 American Chemical Society
Published on Web 07/13/2007

TABLE 1: Excitation Energies (eV) for the Transitions to Excited Singlet Electronic States of the Si_2H_6 and Ge_2H_6 Molecules (geometry optimization has been carried out at the B3LYP/6-311G* level; the B1 basis set is LanL2DZ + 0.246(d) + 0.03, 0.01(sp) for Ge Atoms and 6-31G* for O and H)

system, method	2^1A_g	1^1B_u	1^1A_u, 2^1B_u
Si_2H_6, EOM-CCSD/6-311+G*	7.72[a]	7.99	8.16
Ge_2H_6, EOM-CCSD/aug-cc-pVTZ	7.24	7.46	7.72
Ge_2H_6, EOM-CCSD/B1	7.25	7.56	8.09

[a] The experimental value is 7.6 eV, from ref 33.

being quite suitable for Si, it is insufficient for Ge, as it contains only two contracted Gaussians for the valence orbitals. On the other hand, the 5.06 eV absorption band assigned to GeO_2−OV[13] seems to have too low energy as compared to the corresponding value for SiO_2−OV. Obviously, this question requires a more careful investigation.

It was pointed out[24] that the S_0−S_1 excitation energies for SiO_2-related OV and the Si_2H_6 molecule are similar. As we have not found the respective experimental value for the Ge_2H_6 molecule, we calculated it here at the EOM-CCSD level with Dunning's aug-cc-pVTZ basis set (Table 1). The excitation energy for Si_2H_6 computed using this approach is in good agreement with the experimental value, 7.7 vs 7.6 eV, respectively, so we expect the accuracy for Ge_2H_6 to be similar. The calculated energy of the S_0−S_1 transition is ~0.5 eV lower for the Ge−Ge bond as compared to the Si−Si bond; thus, it is reasonable to expect a similar difference for excitation energies in GeO_2 and SiO_2 OVs. The S_0−S_1 transition energy for OV in GeO_2 can then be estimated as 7−6.5 eV, which is significantly higher than the PE energy used for the activation of PL in GeO_2 nanowires.[1] If this estimate is accurate, one has to invoke a two-photon process for the OV excitation, leading to highly excited Rydberg states with the potential energy properties similar to the positively charged oxygen vacancy, OV^+. It was pointed out[23] that OV^+ has two geometrical configurations with close energy values, a regular structure with an elongated A−A distance (A = Si or Ge) in place of the A−O−A bridge and an inverted ("puckered") configuration with the broken A−A bond and a three-coordinated O atom (see Figure 1). According to the model calculations,[22] potential energy curves of excited singlet states of SiO_2−OV exhibit similar behavior; after gradual de-excitation of Rydberg states, the system descends to either of two different local minima on the S_1 singlet excited-state surface, which can generate two PL bands. The calculated S_1−S_0 emission energies for SiO_2−OV are ~4.3 and 3.3 eV for the regular and inverted forms, respectively.[22] Unfortunately, the inverted structure in that work[22] was simulated by a small model cluster, $(OH)_3Si$−$Si(OH)_3$*OH_2, without geometry optimization. Nevertheless, these results indicated that the inverted OV is a potential candidate to serve as a source of the blue PL band in GeO_2 and should be investigated more carefully.

Another possibility is presented by the double oxygen vacancy. According to the calculations by Pacchioni and Ierano,[24] the S_0−S_1 excitation energy for DOV in SiO_2 is ~1 eV lower than that for OV, and hence we can expect the energy value ~5.5−6 eV for GeO_2. In such a case, the PE energy used to excite luminescence in GeO_2 nanowires[1] would be sufficient for single-photon excitation of the observed PL.[1]

All these findings indicate that OV and especially DOV in quartz-like GeO_2 are possible candidates for the formation of the bright-blue PL band.[1] Therefore, the goal of the present work is to investigate the photoabsorption and photoluminescence properties of these defects in quartz-like GeO_2 by means of quantum chemical modeling.

Calculation Details

In quartz-like GeO_2, as in SiO_2, the bonding has a local character, and the influence of a point defect on the electronic distribution is limited to its nearest neighborhood. In the adjacent layers around the defect, the perturbation of electronic density is usually small. This allows one to treat electronic transitions in such defects using cluster models, which were discussed and widely used earlier.[20−32] A model cluster usually includes the atoms directly involved in the electronic redistribution (the active region) and their nearest neighborhood. To avoid the appearance of artificial transitions originating from broken boundary bonds connecting the cluster with the rest of the bulk, hydrogen atoms are usually added to terminate these bonds. It was demonstrated[20,24,27−30] that to properly reproduce the electronic structure and relative energies of excited states, it is sufficient to take into account the defect itself and the oxygen atoms linked to it, for instance, the O−AO_3, O = AO_2, or AO_2 fragments for the O−A, O = A<, or A< point defects, respectively. Normally, surface point defects, such as the nonbridging oxygen (NBO), peroxy radical, surface E′−center, or two-coordinated Si or Ge, do not cause substantial distortion of the network. For model clusters simulating such systems, full geometry optimization is usually carried out and symmetric structures corresponding to the local symmetry of the defects are used in most cases.

Alternatively, defects involving oxygen vacancy are able to deform the network, mainly because of mechanical distortions of the defect itself and its surrounding fragments. In order to simulate both network relaxation caused by the defect and its incorporation into the bulk in such systems, one needs to use larger model clusters, which include at least one additional layer of bonds around the defect. The atomic coordinates inside the model cluster should be optimized to simulate the network relaxation, whereas the positions of the boundary atoms should be kept frozen in order to mimic the situation in which the defect is embedded into the bulk. The positions of boundary atom are usually determined from larger defect-less clusters or are taken from the crystallographic data. The large model clusters usually do not exhibit any symmetry higher than C_1.

Our theoretical approach to model OV and DOV in GeO_2 is similar to that employed earlier to simulate point defects in SiO_2 of the same type,[22−24] except that we used larger clusters, which included a point defect itself and one or two −O−Ge layers with boundary Ge atoms around them. The oxygen vacancy itself causes relatively moderate distortion only in the nearest vicinity affecting mainly the Ge−O−Ge bond angles around OV. Therefore, for the regular ground state structure it will be possible to use the X_3Ge−GeX_3 (OV) or X_3Ge−GeX_2−GeX_3 (DOV) clusters, where X = $OGeH_3$. However, the inverted configurations and excited states of OV and DOV can cause more substantial reconstruction of the network, and therefore, the ground state optimization was performed with much larger clusters, including an additional layer around the active region (Figure 1). The OV and DOV model clusters were designed to simulate the ground singlet and the lowest triplet states for single and double oxygen vacancies, whereas the OV′ cluster was constructed to model the inverted OV. The coordinates of boundary atoms were fixed at the crystalline positions and the boundary Ge− bonds connecting the defect vicinity with the rest of the bulk were terminated by H atoms. Smaller model clusters were used for calculations of excitation energies for photoabsorption (Figure 2), where the atomic coordinates were

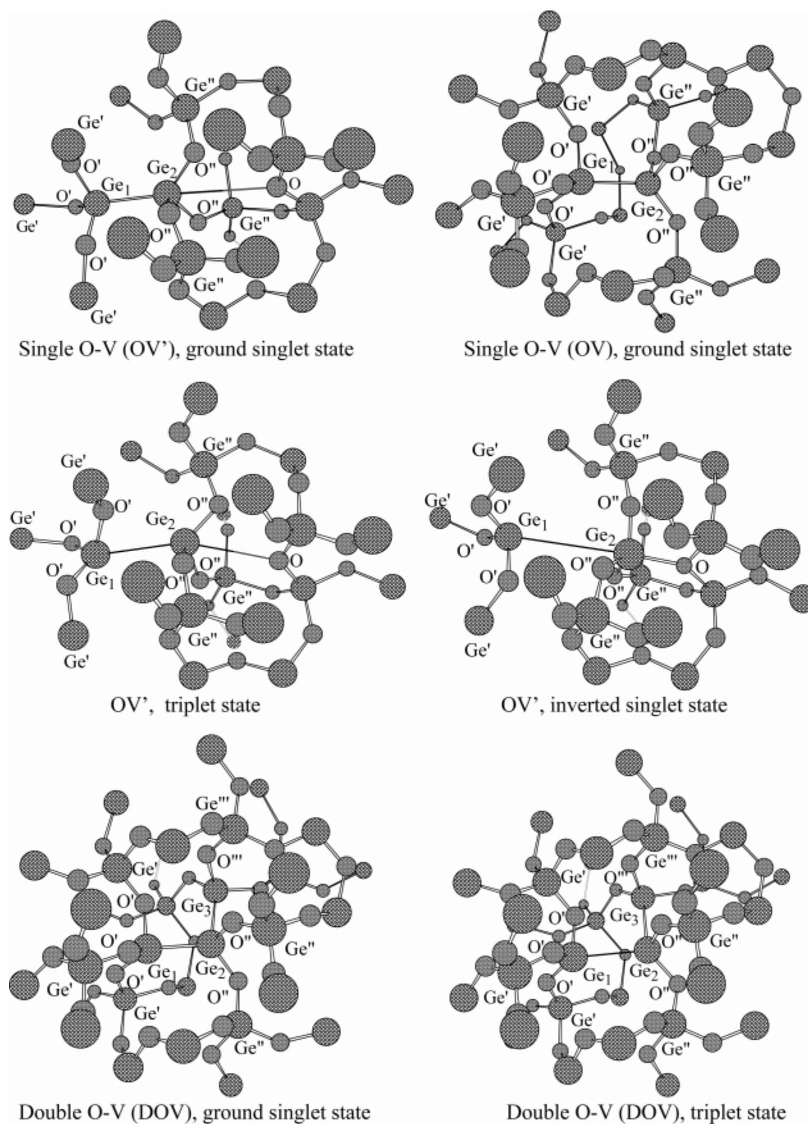

Figure 1. Model clusters used for simulation of the ground singlet and triplet states of single and double oxygen vacancies (OV and DOV) in quartz-like GeO_2. Terminal hydrogen atoms are not plotted.

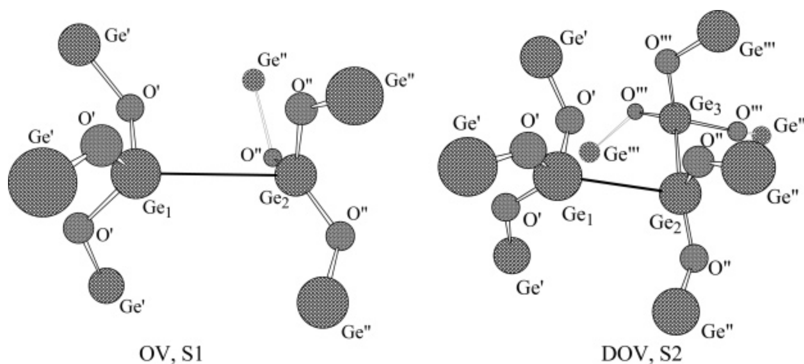

Figure 2. Model clusters used for simulation of excited singlet states of single and double oxygen vacancies (OV and DOV) in quartz-like GeO_2. Terminal hydrogen atoms are not plotted.

taken from the large clusters (OV and DOV in Figure 1) simulating the ground states of the defects. The same models were used to optimize excited-state geometries, except the positions of boundary atoms were taken from the optimized geometries of the larger clusters in the lowest triplet state, because the structures of the triplet and lowest excited singlet states are expected to be similar in these systems.

Geometry optimization for the ground states of model clusters was carried out at the hybrid density functional (DFT) B3LYP[34−36] level of theory with the LANL2-DZ basis set augmented by polarization d-functions with the corresponding effective core potential[36,37] for Ge atoms and the 6-31G* basis set for O and H. We demonstrated earlier[31] that this approach reproduces geometric parameters in GeO_2-related systems reasonably well. For calculations of excited states, this basis set was augmented with a d polarization function (0.246) and two diffuse s- and p-functions (0.03, 0.01) on Ge atoms in the active region of the cluster. For boundary Ge atoms, we used

TABLE 2: Optimized Interatomic Distances for the Clusters Simulating a Single Oxygen Vacancy (OV) in Quartz-Like GeO_2

	Ge_1-O'	Ge_1-Ge'	Ge_1-Ge_2	Ge_2-O''	Ge_2-Ge''	Ge_2-O
OV′, S_0	1.76−1.77	3.18−3.27	2.53	1.77−1.78	3.04−3.19	3.86
OV, S_0	1.75−1.77	3.06−3.22	2.48	1.75−1.77	3.15−3.23	
OV′, T_1	1.86	3.11−3.36	3.14	1.77−1.78	2.91−3.16	3.37
OV, T_1	1.76−1.79	3.03−3.15	3.27	1.77−1.79	3.09−3.18	
OV′, inv.	1.75−1.76	3.02−3.21	4.34	1.69−1.72	3.05−3.25	2.0[a]
OV, S_1	1.75−1.84	3.07−3.20	3.71	1.66−1.72	3.00−3.13	
OV, S_2	1.75−1.83	3.09−3.19	3.78	1.67−1.70	2.98−3.16	

[a] Parameter frozen during the geometry optimization.

the LANL2-DZ basis set and the overall basis is designated below as B1. This B1 basis set was tested for several excited states of the Ge_2H_6 system, where the lowest excitations are of similar type as those in OV or DOV: from the Ge−Ge bond to antibonding MOs with substantial contributions from Ge diffuse functions. The aug-cc-pVTZ basis set was used for comparison; for Si_2H_6 the basis set of such quality provides an agreement between the calculated and experimental excitation energy for the first excited-state within ~0.1 eV. (Table 1). According to the calculated results, the energies for the two lowest states computed with the augmented LANL2-DZ (B1) and aug-cc-pVTZ basis sets are in close agreement. Only for the third and fourth excited states does B1 lead to overestimation of the excitation energies by ~0.4 eV (Table 1). Hence, as will be discussed below, in some cases, we also tested basis sets with additional diffuse functions on Ge and O atoms.

Geometry optimization for excited electronic states was performed at the complete active space self-consistent field level (CASSCF or MCSCF[38,39]) with active spaces normally covering molecular orbitals (MO) with occupation numbers from 1.98 to 0.02. Further details will be discussed in consequent sections. As only few valence orbitals are included into the active space, the multireference configuration interaction (MRCI) approach is not very suitable for calculations of transition energies in the systems under investigation because the results are sensitive to the active space. Hence, we employed the closed-shell equation-of-motion coupled clusters EOM-CCSD[38,40] method. In addition, the less sophisticated and less memory- and time-consuming CIS(D)[36,41] approach was also tested. The calculations were carried out using the MOLPRO 2002 and GAUSSIAN 03 program packages.[36,38]

Results and Discussion

1. Ground-State Oxygen Vacancies. Interatomic Ge−Ge and Ge−O distances in Ge−O−Ge bridges calculated for model cluster simulating defectless quartz-like GeO_2 are 3.19−3.21 and 1.74−1.79 Å.[31] In the ground singlet state (S_0) of an oxygen vacancy, the lack of the bridging O atom in one of such links causes significant shortening of the corresponding Ge−Ge distance and leads to the appearance of the direct Ge−Ge interaction with the bond length, which is only 0.1 Å longer as compared to R(Ge−Ge) in Ge_2H_6. The distances calculated in the OV and OV′ clusters are similar; the Ge−Ge bond length is slightly shorter in the larger system, apparently because the OV model cluster is more flexible in comparison with OV′. Ge−O bond lengths are approximately the same in Ge−O−Ge bridges around OV, whereas deviations in Ge−Ge distances are larger, up to 0.1 Å (see Table 2 and Figure 1). Thus, the shift of the vacancy-related Ge atoms is compensated mainly by variations of torsion angles and Ge−O−Ge bond angles. Similar results can be seen also for DOV, but in this case, the Ge−Ge bonds are slightly longer (Table 3). It is worth noting that DOV plus an isolated O_2 molecule lie 6.78 eV higher in energy than the defectless cluster; the relative energy of a cluster with two OV + O_2 is only slightly higher, 6.84 eV. Therefore, the thermodynamic stability of DOV is approximately the same as that of two OV, and both defects should be able to coexist.

In the lowest triplet state (T_1), the Ge−Ge bond is broken and the corresponding Ge−Ge distance is approximately the same as for a regular Ge−O−Ge bridge. This distance is slightly longer in the OV cluster than in OV' (Figure 1, Table 2). In the triplet state, the repulsive Ge−Ge interaction additionally causes some reorientation of the GeO_3 fragments, and the axes of the $Ge_1O'_3$ and $Ge_2O''_3$ pyramids joined together approximately along the Ge_1-Ge_2 direction are slightly rotated with respect to this line (Figure 1). If the Ge_2 atom continues to move in the direction from its position in S_0 to that in T_1, the inverted structure with a three-coordinated O atom (Figure 1) is eventually formed.

Transition energies for the lowest electronic excitations at the ground state (S_0) geometry were computed employing the EOM-CCSD and CIS(D) approaches (Table 4). The calculated energies are similar, with CIS(D) values being slightly lower. According to our results, the excitation energy to the lowest excited singlet state in OV is in the range of 6.7−6.8 eV and this transition exhibits a significant oscillator strength (f); the next two transitions are 0.1−0.3 eV higher in energy and have similar f values. As one can see, the first vertical excitation energy in this case is ~1 eV higher than the PE energy used for PL activation of nanowires,[1] and so excitation of OV is possible only through an indirect non-Frank−Condon transition with low probability or by means of a double-photon process.

In accord with the data reported for SiO_2,[24] in quartz-like GeO_2, the excitation of DOV requires ~1 eV lower energy as compared with that for OV. However, in this case the transition to the second excited-state has the largest oscillator strength, whereas for the third excitation the f value is significantly lower (Table 4). Because the model cluster simulating DOV (Figure 1) is too big for EOM-CCSD calculations, we tested smaller systems, in which some of the terminal $OGeH_3$ groups were replaced by OH (model clusters denoted as C2−C5; see caption in Table 4 for their chemical composition). This replacement has caused moderate variation of calculated energies, but changes in f values for the S_1 and S_3 states calculated for the smaller C3 and C4 clusters were substantial. Therefore, we utilized the C2 cluster, which includes 8 Ge atoms, for EOM-CCSD calculations. For this model, the influence of the cluster size on the calculated results is small; deviations from the excitation energies calculated for the largest C1 cluster are only about 0.05 eV and the oscillator strengths are similar. The extension of the basis set by adding diffuse functions at Ge (s, 0.10) and O (6-31+G*) atoms leads to a small decrease in excitation energies by about 0.1 eV (Table 4).

Using the approximations and models described above, our calculations demonstrate that the PE band at 5.6 eV[1] is able to activate at least two excited states in the DOV defect and that the transition to the S_2 state has a large oscillator strength and therefore is highly probable. Both for S_1 and S_2 excited states in DOV and OV, an electron is transferred from molecular orbitals corresponding to the Ge−Ge bonds to Rydberg-type orbitals with an antibonding Ge−Ge character. As a result, the excitation to these electronic states should lead to the destruction of the Ge−Ge bonds, similarly to the triplet states, with substantial geometry relaxation and large Stokes shifts.

2. Inverted Structure. To obtain preliminary estimates of

TABLE 3: Optimized Interatomic Distances for Clusters Simulating a Double Oxygen Vacancy (DOV) in Quartz-Like GeO_2

	Ge_1-O'	Ge_1-Ge'	Ge_1-Ge_2	Ge_2-O''	Ge_2-Ge''	Ge_2-Ge_3	Ge_3-O'''	Ge_3-Ge'''
S_0	1.76−1.78	3.09−3.24	2.49	1.77−1.78	3.19−3.29	2.51	1.77	3.12−3.21
T_1	1.75−1.79	3.05−3.18	3.12	1.80	3.12−3.30	2.56	1.76−1.77	3.11−3.18
S_1[a]	1.72−1.74	3.13−3.15	3.69	1.75−1.76	3.21−3.29	2.66	1.71−1.77	2.99−3.22
S_2	1.74−1.82	3.10−3.24	3.51	1.71−1.73	3.23−3.29	2.46	1.70−1.73	3.04−3.15

[a] In the region where the S1 potential energy surface crosses with the S0 PES.

TABLE 4: Calculated Excitation Energies (*E*, eV) and Oscillator Strengths (*f*, given in italics) for the Lowest Singlet States of the OV and DOV Defects at the Ground State Geometry (calculations are performed with the B1 basis set, unless mentioned otherwise)[a]

	S_1: E, *f*	S_2: E, *f*	S_3: E, *f*
OV, C, CIS(D)	6.73, *0.347*	6.85, *0.392*	6.96, *0.241*
OV, C, EOM-CCSD	6.81	6.94	7.03
DOV, C1, CIS(D)[b]	5.39, *0.317*	5.72, *0.534*	6.03, *0.094*
DOV, C1, CIS(D)	5.54, *0.390*	5.84, *0.526*	6.17, *0.072*
DOV, C2, CIS(D)	5.58, *0.303*	5.87, *0.516*	6.21, *0.113*
DOV, C2, EOM-CCSD	5.60	5.90	
DOV, C3, CIS(D)	5.48, *0.162*	5.87, *0.680*	6.17, *0.100*
DOV, C4, CIS(D)	5.61, *0.397*	5.80, *0.460*	5.99, *0.203*
DOV, C5, CIS(D)	5.56, *0.027*	5.74, *0.564*	6.07, *0.311*

[a] The notation for model clusters is the following: C, $(H_3Ge'O)_3Ge$-$Ge(OGe''_3)_3$; C1, $(H_3Ge'O)_3Ge-Ge(OGe''H_3)_2-Ge(OGe''H_3)_3$; C2, $(H_3Ge'O)_3Ge-Ge(OGe''H_3)_2-Ge(OH)$; C3, $(HO)_3Ge-Ge(OGe''H_3)_2-Ge(OGe''H_3)_3$; C4, $(H_3Ge'O)_3Ge-Ge(OH)_2-Ge(OGe''H_3)_3$; C5, $(HO)_3Ge-Ge(OGe''H_3)_2-Ge(OH)_3$. [b] Calculated with the B1a basis set, which is obtained from the B1 basis set by adding an s-function on Ge (0.10) and using the 6-31+G* basis set on O atoms.

TABLE 5: EOM-CCSD/B1 Calculated Relative Energies (RE, in eV) for the Lowest Singlet States of the Inverted OV Defect at Different Ge_2-O Distances

	R(Ge_2-O) (Å)		
	2.4	2.2	2.0
RE(S_0)	2.49	2.99	3.22
RE(S_1)	3.36	3.85	3.90
RE(S_2)	5.20	5.58	5.01

the S_0-S_i energy differences for the inverted OV structure, we scanned the potential energy surface (PES) of the inverted OV model cluster in the vicinity of a possible local minimum. According to the results by Pacchioni and Ierano for SiO_2,[22] the distance between the three-coordinated O and inverted Si atoms is close to 2 Å. Because the corresponding R(Ge_2-O) distances (Figure 1) should be longer (the Ge atom is larger than Si) the calculations were carried out at the distances of 2.4, 2.2, and 2.0 Å. For each point on the PES, these values were kept frozen, whereas all other geometric parameters were optimized for the ground singlet state. Next, we calculated relative energies of the lower excited singlet states using the partially optimized geometries at the EOM-CCSD level (Table 5). We found that in this region of the surface, the ground state energy $E(S_0)$ is much higher than that at the equilibrium geometry and that the difference grows rapidly as the $Ge_2-O<$ distance shortens. In contrast, the energies of the excited S_1 and S_2 singlet states are lower than at the ground state geometry (vertical excitation), so it is quite probable that some excited states have a local minimum in this region. However, the S_0-S_1 and S_0-S_2 energy differences calculated at these geometries are rather low, below 1 eV for S_1 and 1.8−2.7 eV for S_2; obviously, optimization of the excited-state geometries will further reduce these value, and thus both S_0-S_1 and S_0-S_2 emission (PL) energies in this region of the PES are expected to be lower as compared to the observed PL band.[1] Therefore, the properties of the inverted OV were not investigated any further.

3. Excited OV and DOV. As in the triplet state, the first singlet excitations for OV and DOV lead to the cleavage of the Ge−Ge bonds. Hence, we started geometry optimization for the S_1 and S_2 states from the optimized T_1 geometry using the $(H_3Ge'O)_3Ge$-$Ge(OGe''_3)_3$ and $(H_3Ge'O)_3Ge$-$Ge(OGe''H_3)_2$-Ge-$(OGe'''H_3)_3$model clusters shown at Figure 2. The positions of boundary atoms were taken from the optimized triplet structure and were kept frozen. Optimization was performed at the CASSCF level with (10,10) or (10,11) active spaces with 10 electrons on 10 or 11 MOs for the S_1 or S_2 states of OV, and (12,11) active space for the S_1 and S_2 states of DOV. These active spaces cover MOs with occupation numbers from 1.98 to 0.02. The active spaces used are rather far from being full and include only MOs corresponding to the Ge−Ge bonds and several lone pairs of the neighboring O atoms; a large portion of valence electrons remains out of the active space. Therefore, the CASSCF approach applied here is unable to take into account a substantial part of electron correlation and to some extent is similar to the HF method for the ground state; although it is likely suitable for the geometry optimization, significant errors can be anticipated for the calculated relative energies.

The first excited singlet state S_1 for OV is formed by an electron transfer from the orbital with the Ge−Ge bonding character to a vacant MO with an antibonding Ge−Ge character and substantial contributions from diffuse functions, mainly s-AOs. Such MOs represent diffuse localized states, which to some extent are similar to lowest Rydberg-type states in molecular systems. At the optimized S_1 geometric configuration, one of the electrons involved in the excitation occupies an orbital best described as a lone pair of the Ge_1 atom, and the other is located predominantly on the Ge_2 atom. The repulsive Ge_1-Ge_2 interaction in this case is more significant than for T_1, and the corresponding Ge−Ge distance is ~0.4 Å longer (Table 2, Figure 1). In contrast, repulsive interactions of these electrons with the Ge−O bonds in the S_1 state are weaker than in T_1; the respective Ge−O distances for T_1 are slightly longer (Table 2). In the second excited singlet state S_2 of OV, the electron-donating MO is the same, but the accepting orbital has substantial contributions of diffuse p-AOs from the Ge_2 center. The antibonding character of this orbital is stronger and the Ge_1-Ge_2 distance in the S_2 state is slightly longer. The other bonds are similar in the S_1 and S_2 states (Table 2).

De-excitation (PL) energies at the optimized geometries of the S_1 and S_2 excited states were calculated at the EOM-CCSD and CIS(D) levels (Table 6); the CASSCF energies and oscillator strengths are also shown in Table 6 for comparison. For these structures, the discrepancies between the energies calculated by different methods are not as small as for the ground state structures. In some cases, the differences between the excitation energies calculated at the CASSCF, CIS(D), and EOM-CCSD levels reach 0.3−0.4 eV, where the CASSCF energies are higher and the CIS(D) values are lower as compared to the EOM-CCSD data. According to the CASSCF results, the wave

TABLE 6: Calculated Relative Energies (*E*, eV) and Oscillator Strengths (*f*, in italics) for the Lowest Singlet States of the OV and DOV Defects at the Geometries Optimized for Excited Electronic States (B1a basis set was used; for CIS(D), the *f* values are calculated at the CIS level)

system, geometry, method	$E(S_1), f(0-1)$	$E(S_2), f(0-2), f(1-2)$
OV, C, S_1, CAS	3.55, *0.525*	
OV, C, S_1, CIS(D)	2.72, *0.797*	4.22, *0.066*
OV, C, S_1, CIS(D)[a]	2.73, *0.757*	4.19, *0.067*
OV, C, S_1, EOM-CCSD	3.08	4.31
OV, C, S_2, CAS	2.90, *0.149*	3.40, *0.390, 0.068*
OV, C, S_2, CIS(D)	2.31, *0.601*	2.98, *0.104*
OV, C, S_2, CIS(D)[a]	2.33, *0.580*	2.96, *0.091*
OV, C, S_2, EOM-CCSD	2.71	3.31
DOV, C1, S2, CAS	2.28, *0.006*	2.94, *0.538, 0.002*
DOV, C1, S2, CIS(D)[a]	1.99, *0.009*	2.19, *0.449*
DOV, C2, S2, CIS(D)[a]	2.10, *0.019*	2.18, *0.421*
DOV, C2, S2, CIS(D)	2.14, *0.035*	2.17, *0.429*
DOV, C2, S2, EOM-CCSD	2.46	2.63

[a] Calculated with the B1a basis set, which is obtained from the B1 basis set by adding an s-function on Ge (0.10) and using the 6-31+G* basis set on O atoms.

functions for the investigated excited states are mainly single-determinant; the coefficients for other determinants do not exceed 0.07−0.05. Nevertheless, the account of electron correlation is very limited in CASSCF, and the CIS(D) and EOM-CCSD methods seem to be more preferable for these states. Also, within the CIS(D) approach, the account of very significant contributions from double excitations is rather approximate and it is not very appropriate for the structures with broken bonds. In our opinion, the EOM-CCSD method with more reliable treatment of double excitations should be the most suitable for the systems we consider here.

According to the results calculated at the EOM-CCSD level, the PL energy from the S_1 and S_2 states of OV, 3.1 and 3.3 eV, respectively, are higher than the observed PL band[1] (Table 6). Taking into account that the direct photoexcitation of OV requires a higher energy than that used for the PL activation in the experiment, we conclude that the optical properties of the OV defect are not suitable to make it a proper candidate responsible for the generation of the PL band observed in GeO_2 nanowires.

In DOV, the first excited S_1 state is formed in the same way as in OV: an electron is removed from the Ge_1-Ge_2 bond and placed to a diffuse antibonding Ge_1-Ge_2 MO with a contribution from diffuse s-orbitals. However, in this case, the accepting MO additionally has an antibonding character for the Ge_2-Ge_3 interaction, and geometry optimization for the S_1 state of the DOV model cluster leads not only to the rupture of the Ge_1-Ge_2 bond but also to the elongation of the Ge_2-Ge_3 distance. In this case, we were unable to locate a minimum on the PES; in the process of geometry optimization, the systems approached the region where the S_1 and S_0 surfaces cross (the energy difference is only ~0.005 eV). In this region (see Figure 2 and Table 3), the convergence of the CASSCF procedure becomes very poor. Nevertheless, on the basis of such behavior of the S_1 and S_0 PES, we can suppose that for the S_1 state of DOV, the de-excitation process proceeds via a radiationless transition through the S_1-S_0 intersection.

For the S_2 state of DOV, the electron accepting MO contains large contributions of diffuse s- and p-AOs mainly from the Ge_2 center and includes antibonding Ge_1-Ge_2 and weak bonding Ge_2-Ge_3 interactions. The optimized structure for this state has geometric parameters similar to those found for the triplet state, but with a longer Ge_1-Ge_2 distance and a shortened Ge_2-Ge_3 bond (Figure 2, Table 3). The calculated relative energies of S_1 and S_2 states at the S_2 optimized geometry together with the corresponding oscillator strength values are presented in Table 6. Similarly to OV, the CASSCF method overestimates and CIS(D) underestimates the energy difference between the ground and excited states. At the most reliable EOM-CCSD level, the PL energy for the $S_2 \rightarrow S_0$ de-excitation is ~2.6 eV; this value is rather close to the peak position of the PL band observed in GeO_2 nanowires.[1] The oscillator strength for the $S_2 \rightarrow S_0$ transition is large and the $S_2 \rightarrow S_0$ de-excitation channel should be highly probable. It is worth mentioning that in the lowest excited states, the displaced electron remains localized mainly around the Ge_2 center, and variations in the basis set and in the cluster size (with conservation of the nearest neighborhood for the Ge_1, Ge_2, and Ge_3 centers) do not cause substantial changes in the calculated properties for this transition (see Tables 4 and 6).

Thus, the optical properties of the DOV defect are in accord with the features of the PL band in GeO_2 nanowires: a double oxygen vacancy in quartz-like GeO_2 is able to adsorb radiation at 5.5−5.7 eV with a high probability, and after geometry relaxation in the excited S_2 state, it can emit light with a large Stokes shift in the energy range of about ~2.6 eV.

Conclusions

The lowest electronic transitions of the OV and DOV defects in quartz-like GeO_2 occur at the energies ~1 eV lower as compared to those for analogous excitations in SiO_2. In particular, for OV in GeO_2, the calculated lowest photoabsorption singlet−singlet transitions have energies of 6.8−7.0 eV and large oscillator strengths, whereas for DOV, such excitations occur in the range of 5.5−5.9 eV. In both systems the lowest excited states are formed by electronic transition from the Ge−Ge bond to Rydberg-type orbitals with an antibonding Ge−Ge character. This leads to the destruction of the Ge−Ge bond and significant geometry reorganization causing a large Stokes shift. As a result, the PL from the first two excited states of OV should take place at 3.1−3.3 eV. The inverted structures of OV, if they exist, would have substantially lower emission energies.

For DOV, de-excitation of the first excited singlet state proceeds in a radiationless manner, whereas the second excited singlet state is calculated to have PL energy of ~2.6 eV and a large value of the oscillator strength. Among all investigated transitions in various point defects in GeO_2, the S_2 state in a double oxygen vacancy seems to be the most suitable candidate to generate bright-blue PL observed experimentally[1] for substoichiometric quartz-like GeO_2: the formation of this state is possible upon absorption of 5.7−5.9 eV photons and the corresponding PL band should be peaked at 2.6 eV, whereas both PA and PL show large oscillator strengths. These properties are in good agreement with the PL features observed in GeO_2 nanowires.

Acknowledgment. The authors acknowledge Academia Sinica and National Science Council of Taiwan, P. R. China, for financial support. Partial support from Florida International University is also appreciated.

References and Notes

(1) Wu, X. C.; Song, W. H.; Zhao, B.; Sun, Y. P.; Do, J. J. *Chem. Phys. Lett.* **2001**, *349*, 210.

(2) Maeda, Y. *Phys. Rev. B* **1995**, *51*, 1658.

(3) Zacharias, M.; Fauchet, P. M *J. Non-Cryst. Solids* **1998**, *227*, 1058.

(4) Pacchioni, G.; Skuja, L.; Griscom, D. *Defects in SiO_2 and Related Dielectrics: Science and Technology*; NATO ASI Series II; Kluwer: Dordrecht, 2000; Vol. 2.

(5) Williams, D. L.; Davey, S. T.; Kashyap, R.; Armitage, J. R.; Ansile, B. J. *Electron. Lett.* **1992**, *28*, 369.

(6) Atkins, R. M.; Mizrahi, V. *Electron. Lett.* **1992**, *28*, 1743.

(7) Mizrahi, V.; Atkins, R. M. *Electron. Lett.* **1992**, *28*, 2210.

(8) Tsai, T. E.; Saifi, M. A.; Friebele, E. J.; Griscom, D. L.; Österberg, U. *Opt. Lett.* **1989**, *14*, 1023.

(9) Lieber, C. M. *Solid State Commun.* **1998**, *107*, 607.

(10) Hu, J.; Odom, T. W.; Lieber, C. M. *Acc. Chem. Res.* **1999**, *32*, 435.

(11) Hosono, H.; Mizuguchi, M.; Kawazoe, H.; Nishii, J. *Jpn. J. Appl. Phys.* **1996**, *35*, L234.

(12) Imai, H.; Arai, K.; Imagawa, H.; Hosono, H.; Abe, Y. *Phys. Rev. B* **1988**, *38*, 12772.

(13) Hosono, H.; Abe, Y.; Imagawa, H.; Imai, H.; Arai, K. *Phys. Rev. B* **1991**, *44*, 12043.

(14) Hosono, H.; Abe, Y.; Kinser, D. L.; Weeks, R. A.; Muta, K.; Kawazoe, H. *Phys. Rev. B* **1992**, *46*, 1145.

(15) Nishii, J.; Fukumi, K.; Yamanaka, H.; Kawamura, K.; Hosono, H.; Kawazoe, H. *Phys. Rev. B* **1995**, *52*, 1661.

(16) Qui, J.; Wada, N.; Ogura, F.; Kojima, K.; Hirao, K. *J. Phys.: Condens. Matter* **2002**, *14*, 2561.

(17) Skuja, L. N.; Streletsky, A. N.; Pakovich, A. B. *Solid State Commun.* **1984**, *50*, 1069.

(18) Trukhin, A.; Poumellec, B. *J. Non-Cryst. Solids* **2003**, *324*, 21.

(19) Skuja, L. *J. Non-Cryst. Solids* **1994**, *167*, 229.

(20) Zhang, B. L.; Raghavachari, K. *Phys. Rev. B* **1997**, *55*, R15993.

(21) Stefanov, B. B.; Raghavachari, K. *Phys. Rev. B* **1997**, *55*, 5035.

(22) Pacchioni, G.; Ierano, G. *Phys. Rev. Lett.* **1997**, *79*, 753.

(23) Pacchioni, G.; Ierano, G. *Phys. Rev. Lett.* **1998**, *81*, 377.

(24) Pacchioni, G.; Ierano, G. *Phys. Rev. B* **1998**, *57*, 818.

(25) Pacchioni, G.; Ierano, G.; Marquez, M. *Phys. Rev. Lett.* **1998**, *81*, 355.

(26) Zyubin, A. S.; Sulimov, V. G. *Glass Phys. Chem.* **1999**, *25*, 144.

(27) Raghavachari, K.; Pacchioni, G. *J. Chem. Phys.* **2001**, *114*, 4657.

(28) Sousa, C.; De Graaf, C.; Pacchioni, G. *J. Chem. Phys.* **2001**, *114*, 6259.

(29) Raghavachari, K.; Ricci, D.; Pacchioni, G. *J. Chem. Phys.* **2002**, *116*, 825.

(30) Zyubin, A. S.; Mebel, A. M.; Lin, S. H.; Glinka, Yu. D. *J. Chem. Phys.* **2002**, *116*, 9889.

(31) Zyubin, A. S.; Mebel, A. M.; Lin, S. H. *J. Chem. Phys.* **2005**, *123*, 44701.

(32) Zyubin, A. S.; Mebel, A. M.; Lin, S. H. *J. Chem. Phys.* **2006**, *125*, 64701.

(33) Itoh, U.; Toyoshima, Y.; Onuki, H.; Washida, N.; Ibuki, T. *J. Chem. Phys*. **1986**, *89*, 4867.

(34) Becke, A. D. *J. Chem. Phys.* **1993**, *98*, 5648.

(35) Lee, C.; Yang, W.; Parr, R. G. *Phys. Rev. B* **1988**, *37*, 785.

(36) Frisch M. J.; Trucks, G. W.; Schlegel, H. B.; Scuseria, G. E.; Robb, M. A.; Cheeseman, J. R.; Montgomery, Jr., J. A.; Vreven, T.; Kudin, K. N.; Burant, J. C.; Millam, J. M.; Iyengar, S. S.; Tomasi, J.; Barone, V.; Mennucci, B.; Cossi, M.; Scalmani, G.; Rega, N.; Petersson, G. A.; Nakatsuji, H.; Hada, M.; Ehara, M.; Toyota, K.; Fukuda, R.; Hasegawa, J.; Ishida, M.; Nakajima, T.; Honda, Y.; Kitao, O.; Nakai, H.; Klene, M.; Li, X.; Knox, J. E.; Hratchian, H. P.; Cross, J. B.; Bakken, V.; Adamo, C.; Jaramillo, J.; Gomperts, R.; Stratmann, R. E.; Yazyev, O.; Austin, A. J.; Cammi, R.; Pomelli, C.; Ochterski, J. W.; Ayala, P. Y.; Morokuma, K.; Voth, G. A.; Salvador, P.; Dannenberg, J. J.; Zakrzewski, V. G.; Dapprich, S.; Daniels, A. D.; Strain, M. C.; Farkas, O.; Malick, D. K.; Rabuck, A. D.; Raghavachari, K.; Foresman, J. B.; Ortiz, J. V.; Cui, Q.; Baboul, A. G.; Clifford, S.; Cioslowski, J.; Stefanov, B. B.; Liu, G.; Liashenko, A.; Piskorz, P.; Komaromi, I.; Martin, R. L.; Fox, D. J.; Keith, T.; Al-Laham, M. A.; Peng, C. Y.; Nanayakkara, A.; Challacombe, M.; Gill, P. M. W.; Johnson, B.; Chen, W.; Wong, M. W.; Gonzalez, C.; Pople, J. A. *Gaussian 03,* revision B.03; Gaussian, Inc.: Pittsburgh, PA, 2003.

(37) Hay, P. J.; Wadt, W. R. *J. Chem. Phys.* **1985**, *82*, 270.

(38) Werner, H.-J.; Knowles, P. J.; Amos, R. D.; et al. *MOLPRO*: *a package of ab initio programs.*

(39) Werner, H.-J.; Knowles, P. J. *J. Chem. Phys.* **1985**, *82*, 5053.

(40) Hampel, C.; Peterson, K.; Werner, H.-J. *Chem. Phys. Lett.* **1992**, *190*, 1.

(41) Head-Gordon, M.; Maurice, D.; Oumi, M. *Chem. Phys. Lett.* **1995**, *246*, 114.